Int. J. Electrochem. Sci., 8 **(2013)** 8019 - 8029

International Journal of
ELECTROCHEMICAL
SCIENCE
www.electrochemsci.org

A Novel Nano-Structured Si-Cu_2O Composite Electrode for High-Capacity Lithium-Ion Battery

Ruoxu Lin, Shichao Zhang[*]*, Guanrao Liu, Zhijia Du, and Libin Kang*

School of Materials Science and Engineering, Beihang University, P. R. China.
[*]E-mail: csc@buaa.edu.cn

Received: 1 April 2013 / *Accepted:* 13 May 2013 / *Published:* 1 June 2013

An improved structure of nano-sized Si-Cu_2O composite material has been obtained employing solvothermal method. The enhanced silicon-copper electrode of higher conductivity has been produced by further electrochemical reduction. The charge-discharge curves, cycling performance were analyzed in detail. The first charge/discharge profile behaviour of silicon-cuprous oxide was also discussed. The composite electrode can accommodate the serious volume expansion of silicon nano particles and strengthen the electrical contact between active silicon and copper foil substrate. The electrode exhibits a high efficiency of 97.9% in 57th cycle afterwards and a capacity retention of 80.2% after 60 cycles with an average fading ratio of ~0.33%.

Keywords: lithium-ion battery, silicon, cuprous oxide, anode

1. INTRODUCTION

In the past two decades the application of silicon as anode in lithium-ion batteries is becoming a promising way due to its correspondingly high theoretical specific capacity of ~ 4200 mAh g^{-1} ($Li_{22}Si_5$) in the field of electrochemical energy storage. Lithium-ion batteries with excellent performance is of long-life span, high charge/discharge rate and high capacity retention after numbers of cycles[1-3]. As anode materials, silicon can relatively fulfil the requirements of appealing capability in intercalation of lithium ions, but meanwhile bring up with poor cyclic stability for its severe volume extension (200%~300%) and disintegration process. Pulverization and cracking occur inevitably caused by lithiation/ de-lithiation of silicon. It leads to an enormous capacity fading and short-life span because of the serious disconnection between active silicon particles/films and current collector[4,5].

Research was conducted on the disadvantage of lithium-ion battery with silicon anode for prolonged cycling and thereby many approaches were taken into account and carried out to solve the

problem during cycling behavior. Micro/nano-scaled silicon-carbon/CMC composite particles were widely used in early times, which resulted in a relatively high stable cycling capacity and a low fading to a certain extent[6-8]. The main loss of the specific capacity in composite powder anode was that decrystallization of silicon powder led to a drastic pulverization in its first cycle, which caused the detach of active materials from substrate and the additives. And then, the composite anode could still not make a better electrical and structural supporting efficiently in subsequent cyclings.

Here the authors report a new structure that cuprous oxide does not act as an active materials in battery but constructional and conduct materials when the cut-off voltage is controlled below ~2.6 V at which elementary copper can not be oxidized into cuprous oxide again. Previous research showed that cuprous oxide, owing to its reduction/oxidation process exists in discharge/charge courses in lithium-ion battery as equation follows (reaction 1), was employed unusually as anode materials with a specific capacity of ~250 mA h g^{-1}[9]:

$$Cu_2O+2Li^{+}+2e^{-}\leftrightarrow Cu+Li_2O \qquad (1)$$

Figure 1 shows the concept of pre-prepared mixture of nano-scaled silicon and cuprous oxide particles and the change after an integrate discharge/charge process between 1.5 V and 0.005 V vs. Li+/Li at a certain rate. These two kinds of nano-sized particles are synthesized by in situ solvothermal method to make a better connection as anode materials. Surface of nano-sized cuprous oxide particles is well deoxidized mostly if a slow discharge rate is set in the first cycle and the 50 nm silicon particles are guaranteed to merge in the new matrix formed by pure copper and lithia for a strong contact. Copper, reduced from cuprous oxide, is an ideal structural support strengthening the conductivity between silicon powder the active materials, and copper foil the substrates due to its structural strength and good performance on electron transport kinetics. At the same time, volume expansion of silicon can be well attenuated, which is attributed to the synergistic effect of the composite materials. This composite prepared of new structure shows an impressive results with respects to its comparatively high reversible charge/discharge capacity, low irreversible capacity and good performance on capacity retention.

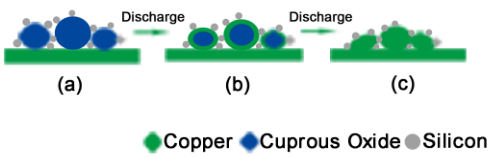

Figure 1. Diagram of structure of pristine silicon-cuprous oxide composite (a), composite electrode discharged during first cycle (b) and composite electrode discharged completely (c).

2. EXPERIMENTAL

Cu_2O powder was synthesized by solvothermal method related elsewhere[10] to obtain different particles in several crystal forms. Nano-sized silicon particles (average size of 50 nm) were

purchased form Hefei Kaier Nanometer Energy & Technology Co., Ltd. The nano-sized particles were dispersed in glycol in which cupric nitrate dissolved to make sure that silicon and cuprous oxide nano particles could be close enough in the course of *in situ* reduction, which avoided the bad attachment between these two kinds of particles if only a simple ball-milling method was applied. The mixture was stirred moderately (200 rpm) and heated at 180 °C for 4 hours under protective atmosphere of nitrogen. Cuprous oxide (average size of 200 nm)-silicon composite obtained was washed by absolute ethyl alcohol and acetone for several times and dried in vacuum oven at 80 °C for 12 hours. The anode materials, prepared by solvothermal method, was consisted of 16.67 wt% silicon nano-particles and 83.33% wt% cuprous oxide nano-particles. The anode slurry was determined to be ~72.73 wt% of composite active materials in which carbon black was of ~18.18 wt% and polyvinylidene fluoride (PVDF) was of ~9.09 wt% using N-methyl pyrrolidone (NMP) as solvent, which was overlaid on copper foil. And then the electrode was heated in vacuum oven at 120 °C overnight before moving into glove box filled with argon gas for half cell assembling. To make a comparison of mixed nano-particles, pure nano-silicon anode (~72.73 wt% silicon, ~18.18 wt% carbon black, ~9.09 wt% PVDF) was also prepared and tested in half-cell simulation.

The half cells were assembled in an argon-filled glove box (MB-10-G with TP170b/mono, MBRAUN) with lithium sheets as counter electrodes. Electrolyte was 1 M LiPF6 in a mixed solution of EC and DEC (1:1 in volume ratio) and membrane separator (Celgard® 2300) was in use. Cyclic voltammogram method was tested by Chenhua® 1100D work station and the cells were tested at different cycling rate between 0.005 V and 1.5 V using Neware® battery test station. The morphology and crystal structure of samples were characterized using a scanning electron microscopy (SEM, Hitachi S-4800) and a transmission electron microscopy (TEM, JEOL JEM 2100F) with an energy dispersive X-ray analyzer (EDS), and X-ray diffraction (XRD, RigakuD/Max-2400), respectively.

3. RESULTS AND DISCUSSION

Figure 2 shows the X-ray diffraction analysis of the cuprous oxide-mixed silicon composite to determine the phase transition before and after cycling. Pattern (a) refers to the original sample without any electrochemical treatments, from which two crystalline phases are observed: solid diamond for crystalline silicon particles and hollow triangle for cuprous oxide. After the first cycle, pattern (b) suggests an evident variation that the peaks of silicon and cuprous oxide disappear, but instead peaks of copper marked by solid circle come into beings. For silicon, it has been reported that crystalline silicon shows volume change with a lattice breakage caused by phase transition in the course of discharge process below 0.3 V, which is indicated to be an irreversible process in subsequent cycles[11,12]. Therefore, the XRD pattern proves well that majority of the Cu_2O particles turn into elemental copper without a reverse reaction if the cut-off voltage is set at 1.5 V vs. Li+/Li far below 2.6 V. It should be noticed that there is still a tiny peak of Cu_2O occurring after the first cycle (marked by arrow), which could be a result from the incomplete reduction of cuprous oxide caused by the tough infiltration path for lithium ions' transporting during the first cycle. The unexpected peak may also be

caused by a multi-step electrochemical reaction of CuO (from substrate) can be described as follows[13]:

$$CuO+xLi^{+}+xe^{-} \rightarrow Cu_{1-x}Cu_xO_{1-x/2} + x/2Li_2O \quad (2)$$

$$Cu_{1-x}Cu_xO_{1-x/2}+(1-x)Li^{+} + (1-x)e^{-} \rightarrow 1/2Cu_2O+(1-x)/2Li_2O \quad (3)$$

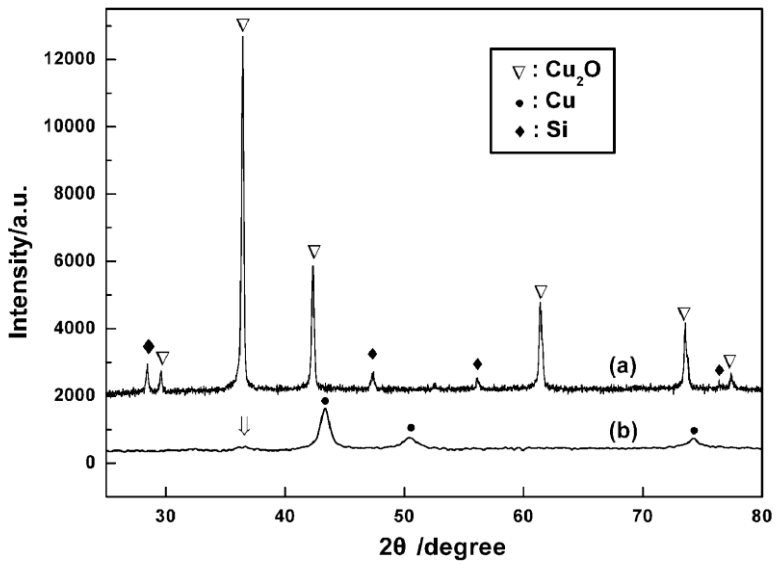

Figure 2. XRD patterns of the composite electrode before (a) and after (b) cycling.

To make a better understanding of the mechanism of phase transition during charge and discharge, a cyclic voltammogram (scanning rate of 80 μV s^{-1}) analysis of composite anode was carried out and the result is shown in Figure 3. During the first discharge (lithiation process), there is a strong cathodic peak (Pa) at around 1.25 V, which disappears in the subsequent cycles. This cathodic peak ranged from 1.5 V to 1.0 V can be assigned to the reaction mentioned above that cuprous oxide turns into elemental copper during the first cycle. A broad peak b (Pb) locating at 0.7 V, which can be observed in the following two cycles, is mainly ascribed to the formation of solid electrolyte interface (SEI) and the decomposition of electrolyte on the silicon surface[14,15]. Ordinarily, peak b disappearing after the first cycle, makes it a difference from the fact that figure 3 shows. It can be explained by previous work that the weak broad peak originates from two reasons: one is deeper Li^{+} intercalation of Cu_2O in minority, and the other is formation of SEI on new surface of nano particles formed from the disintegration of cuprous oxide and crystalline silicon motivated in the following cycles[16]. Lithium-silicon alloying begins at the potential of around 0.28 V and the discharge current continually increases until it reaches to 0.08 V. There comes a visible turning at approximately 70 mV and the current increases drasticlly till the end of discharge, which is attributed to the phase transition of crystalline silicon. In the next two discharges, the potential drops rapidly to a potential of 0.3 V, and then decreases to 0.005 V gradually, which results from the alloying of lithium and amorphous silicon.

Upon charge, current peaks appearing at about 0.37 V and 0.51 V, is consistent with previous experiments on amorphous silicon film anodes[17]. At the same time, voltage fluctuation from 1.0 V to 1.5 V is mainly due to the deformation of SEI and this inevitably plays a part of the charge capacity.

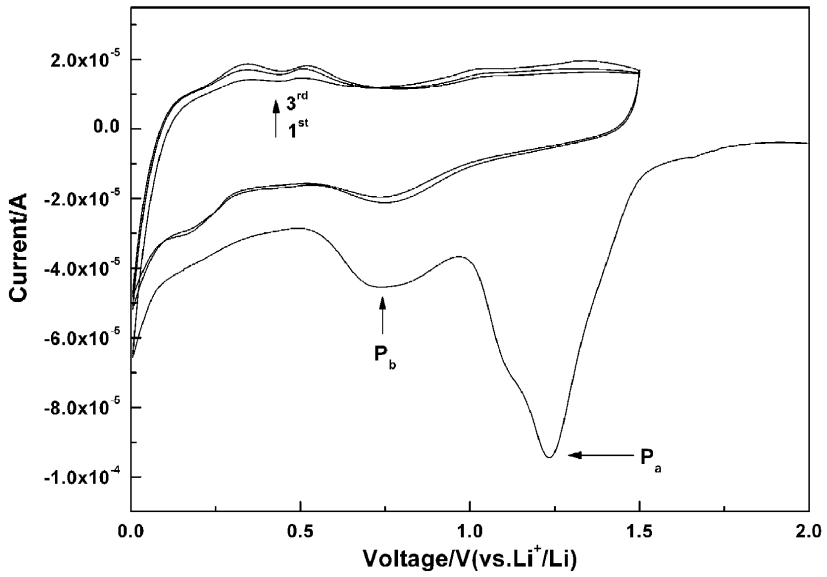

Figure 3. Cyclic voltammogram of a composite Si electrode at a scan rate of 0.08 mV s^{-1} (voltage range: 0.005 V–1.5 V) for the first 3 cycles.

Figure 4 shows voltage profiles of the composite anode based on copper substrate after 5 cycles over a voltage range of 0.01-1.5 V at a current density of 0.42 A g^{-1} (rate = 0.1 C). The first discharge has a sloping region at around 1.5 V and gradually drops to 1.0 V, which is related to lithium ions' intercalating into Cu_2O and the reduction of oxide. The following sloping region ranges from 1.0 V to 0.55 V corresponding with the irreversible capacity (up to 120 mA h g^{-1}) from decomposition of electrolyte and formation of SEI[18]. Then, the third plateau appears at around 0.2 V and drops slowly to the end at 0.01 V, which is assigned to silicon lithiation to crystalline silicon with a phase transition that crystalline changes into amorphous. The total irreversible capacity (up to 570 mA h g^{-1}), mainly consisting of reduction reactions and formation of SEI, plays an important role in the first cycle. Meanwhile the following charge and discharge profiles show typical behavior of lithium intercalation /extraction into/from the amorphous Li_xSi. Although the capacity loss mainly from irreversible intercalatioin of Li-ions makes a big portion during the first discharge, the curves become almost overlapping for the following 4 cycles, suggesting the excellent cycleability of Si-Cu composite electrode. After several cycles, the discharge plateaus can also be observed obviously, indicating the stable amorphous structure of Si film.

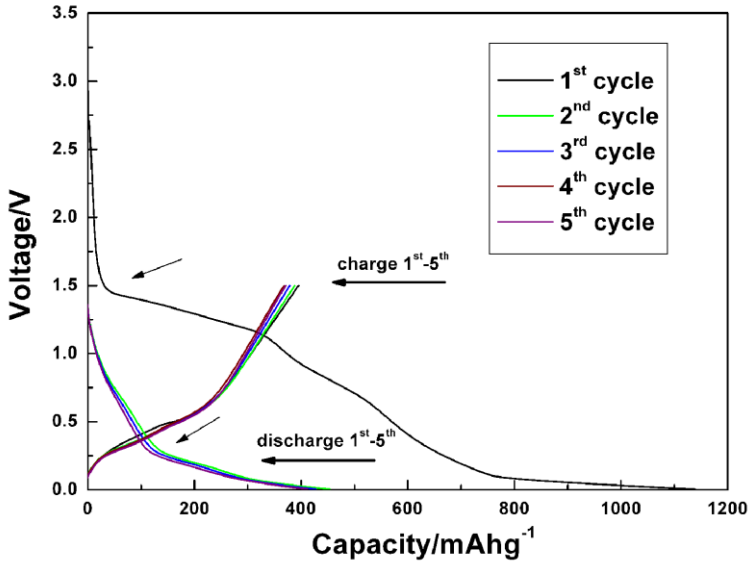

Figure 4. Voltage profiles of the composite electrode cycled between 0.01 and 1.5 V versus Li^+/Li at a rate of 0.1 C (0.42 A g^{-1}).

Figure 5 depicts the top-view of nano-scaled cuprous oxide-silicon composite electrode before and after a 60-cycled half-cell test. Specimen tested for 60 cycles was disassembled and the electrode was filtered with EC and acetone for several times, of which the morphology was determined by scanning electron microscopy (SEM). Owing to the solvothermal method, the scale of the nano cuprous oxide particles was limited with a short range of ~100-200 nm that led to a preferable porosity for a better infiltration of electrolyte. The composite of these two kinds of nano-particles was well proportioned. As is shown in figure 5a, the mixed powder of cuprous oxide and nano-sized silicon both give a relatively bright portrait means that an unfavourable electrical contact exists without the reduction of cuprous oxide. It is hard to distinguish clearly cuprous oxide particles or silicon particles both in SEM and TEM (inset image in figure a) for a tight contact of nano particles due to solvothermal method. In figure 5b, the electrode materials show a tiny shrinkage resulting from the pulverization in charge cycles of a ranged scale of ~30-50 nm, and at the meantime the surface was consisted of copper (supported by figure 6) with good conductivity. Previous work shows that a disintegration happens when Cu_2O is cycled for several times and particles will break into smaller ones[16], which can be an explanation of the formation of SEI on new surface of particles at around 0.75 V after the first cycle. Of similar sizes, both nano particles integrated provide with a more convenient path for electrolyte, and result in a synergistic effect for composite anode consisting of active materials (silicon) and inactive materials (copper and Li_2O). Therefore, the new structure not only facilitates the electron transportation, but also acts as a strengthened framework to spread or release the inner stress of silicon nano particles embedded by restricting the huge volume expansion.

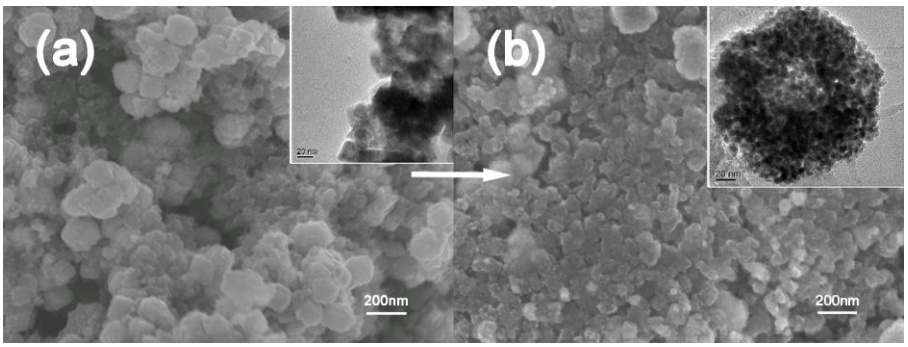

Figure 5. Morphology of electrode's surface before cycling (a) and after cycling (b).

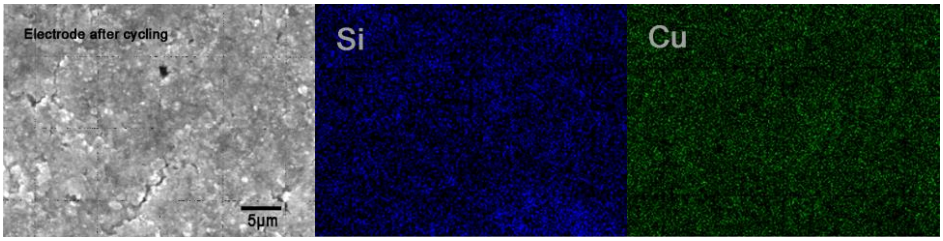

Figure 6. Elemental Si and Cu EDX maps of electrode surface after 60 cycles.

To better study the mechanism of the improvement of the cuprous oxide-mixed silicon anode, electrochemical impedance spectroscopy (EIS) was employed to determine the changes of resistance in anode after series of cycle numbers. For impedance measurement, half-cell system was tested using lithium foil as a counter electrode and the explored frequency range was from 100 kHz to 100 mHz under ac stimulus with 10 mV of amplitude and no applied voltage bias. Figure 7 shows the comparison of different five statements of Nyquist plots simulations after 0, 1, 5, 10 and 50 discharge/charge cycles, respectively. At lower frequencies (below 10 Hz) the plot fits a similar slope of the curves results from the lithium-ions moving into bulk anode materials smoothly and the electrode is still remaining porous with small amount of pulverization of silicon particles. It is propitious to the transportation of Li-ions from electrolyte into inner layers of anode. We thereby focus on the obvious change at high and medial frequencies between 100 kHz to 10 Hz at which the electronic contact between substrate and active materials, the ohmic contact due to appearance of copper-silicon interface, electron transfer resistance on the electrode interface and a passivated SEI layer dominates. Changes of the length of semicircle's diameter of Nyquist plots for different number of cycles can be observed in this picture. It has a tendency that the semicircle is becoming smaller with 5 to 50 cycling numbers except the second plots (red marks) upon the first cycle. The irregular increase of the resistance of the anode materials after the first cycle is ascribed to a sophisticated cause consisting of the aggregation of Li_2O created, an incomplete reduction of cuprous oxide particles in deep layer and the formation of SEI layers during the first cycle, which leads to an unfavourable electrical contact in internal active materials[19,20]. With several cycles the electrolyte can infiltrate into deeper layers in porous anode gradually and cuprous oxide powders closed to substrate can be

well deoxidized and make a good contact to copper foil enhancing the nano-sized silicon of weak conductivity simultaneously that decrease the resistance of electrode efficiently[21]. As is shown in this image, the plot after 50 cycles overlap the one after 10 cycles well, which means that the composite electrode becomes stable for a better conductivity after around 10 cycles.

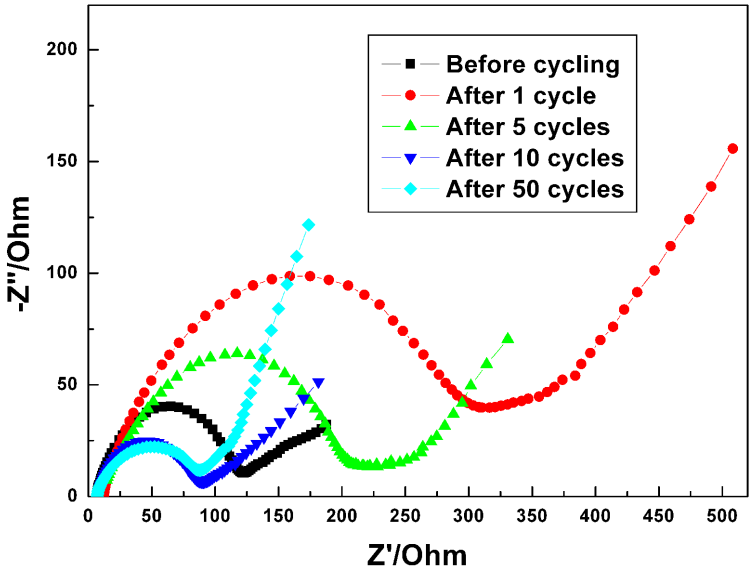

Figure 7. Voltage profiles of the composite electrode cycled between 0.01 and 1.5 V versus Li^+/Li at a rate of 0.1 C (0.42 A g^{-1}).

Pure silicon electrode with carbon black as conductivity and PVDF as bonding materials mentioned above was utilized in half-cell tests to determine the change in composite electrode after nano-scaled Cu_2O particles were taken advantage of. Both cells were charged and discharged at a rate of 0.1 C (0.42 A g^{-1}), respectively. The plots of specific charge capacity and coulombic efficiency are shown in figure 8. It should be noticed that the theoretical capacity of composite will be ~665 mA h g^{-1} (Cu_2O:Si =5:1) marked by dashed line. As the former type of cell concerned, the first discharge and charge specific capacity of pure silicon electrode are 2212.5 and 403.3 mAh g^{-1}, respectively, with a very low initial coulombic efficiency of ~18.22%. The huge irreversible capacity ratio of 81.78% at the first cycle could be assigned to the formation of SEI layers on surface of nano-scaled silicon particles, the deformation of lithium salts in the course of discharge and charge, and unfavorable electrical disconnection caused by pulverization of silicon powder for its uncontrollable volume expansion[22]. In the following cycles, the efficiency increases gradually and can hold to ~73.5%, whereas the total electrode can only provide the charge capacity of silicon of ~188 mA h g^{-1} owning to small amount of active materials clung to the collector. Therefore, the half cell can not perform electrical activation after 20 cycles. The new structure of composite electrode shows a visible improvement on cyclic stability and capacity retention in half cell test both in figure 8 compared to pure silicon electrode. As can be seen in image, the impressive amount of 555.7 mA h g^{-1} is liberated from composite part of

electrode upon delithiation at the first cycle and the irreversible capacity ratio is kept about 51.9% originated from the main causes mentioned above. We noticed that the coulombic efficiency increases in the next 11 cycles, which is possibly ascribed to the activation of silicon powder in deep layer by electrolyte infiltrating gradually and the formation of enhanced matrix of active and inactive materials[23,24]. The cycling becomes stable from the 11th discharge/charge process with close value of efficiency (ca. 96 % for cycles 11-35, ca. ~97 % for cycles 36-60), which can be originated from the fact that metal copper provides enough electrical connection with active materials, thereby shortening the diffusion distance of Li-intercalation, accompanied with a convenient collecting and transporting of electron. The cell exhibits an increased coulombic efficiency in most of the discharge/charge process and high efficiency of 97.9% in 57th cycle afterwards and also a capacity retention of 80.2% after 60 cycles with an average fading ratio of ~0.33%.

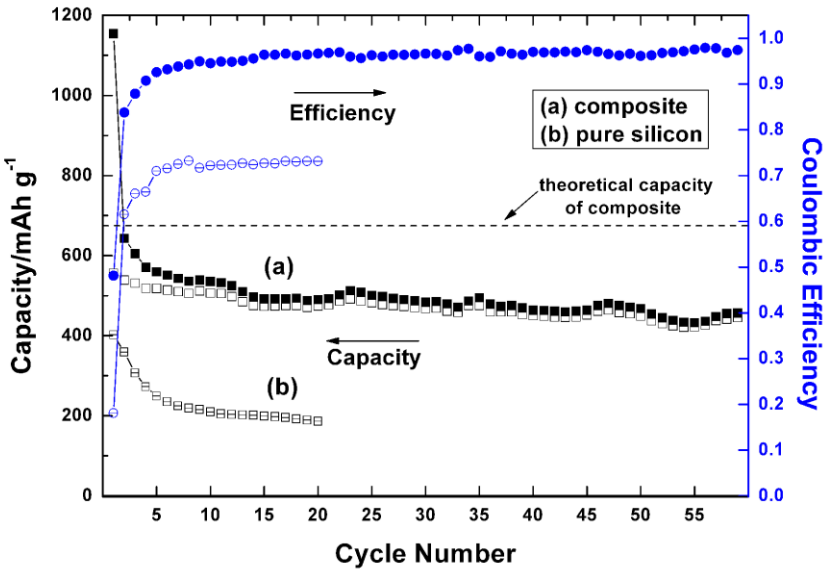

Figure 8. Cyclic behaviour of pure silicon electrode and composite silicon electrode.

Figure 9 shows the comparison of charge/discharge capacity of silicon in composite anode at different rate in every five cycles of 0.05 C, 0.1 C, 0.5 C, 1 C, 2 C and back to 0.1 C, respectively. Slow rate of 0.05 C (210 mA g^{-1}) was operated in the first five cycles to enhance the stability of composite electrode and provide a good condition for lithiation and delithiation process in the following cycles. The charge capacity of silicon starts with 2340.7 mA h g^{-1} and retains 2203.8 mA h g^{-1} with a capacity retention of 94.1%, and meanwhile can still maintain an excellent results of 1851.9 mA h g^{-1} with a retention of 99.4% at the rate of 0.1C and of 1307.0 mA h g^{-1} with a retention of 92.5% at the rate of 0.5 C, respectively. There is a capacity drop of ~15.6% when the cycling rate increases from 0.5 C to 1 C with an average charge capacity of ~1102.2 mA h g^{-1} in five cycles. A favourable specific charge capacity of silicon above 580.2 mA h g^{-1} is illustrated in the image, which means a good stability of electrode materials at a high rate of 2 C (8.4 A g^{-1}) attributed to the structure of nano silicon fusing in reduced Cu_2O particles. The strengthened framework making a connection between active materials and current collector fits the results as well in other more cycling tests.

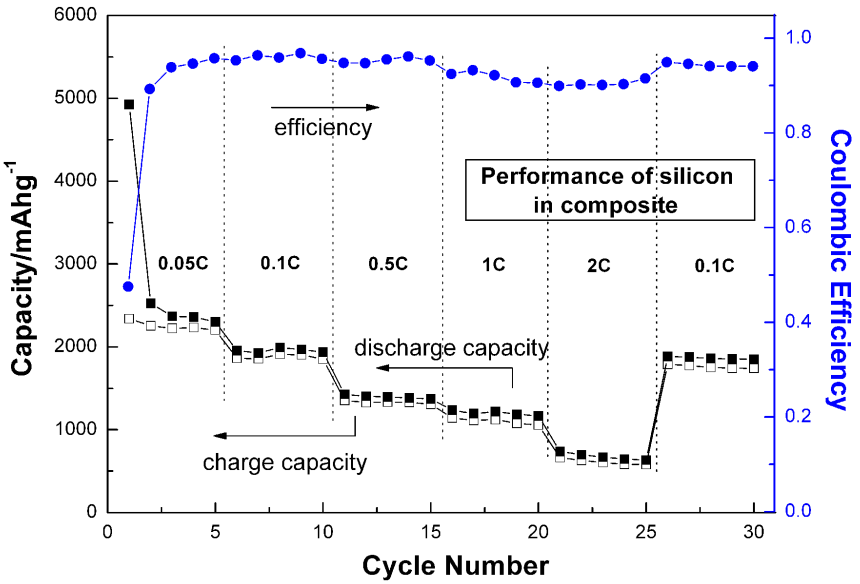

Figure 9. Specific capacity and coulombic efficiency of composite electrode at rate of 0.05 C, 0.1 C, 0.5 C, 1 C and 2 C.

4. CONCLUSIONS

In conclusion, a novel type of structure, described as nano-scaled silicon-copper composite, reduced from cuprous oxide-silicon mixture, served as anode materials, was successfully synthesized for lithium-ion battery. The composite electrode could accommodate the serious volume expansion of silicon nano particles and enhance the electrical contact between active silicon and copper foil substrate, and improve the electrochemical performance of silicon-contained anode. The electrode exhibits a high efficiency of 97.9% in 57th cycle afterwards and a capacity retention of 80.2% after 60 cycles with an average fading ratio of ~0.33%. The optimized content of silicon and cuprous oxide powders in composite electrode and the precise micro-mechanism will be further investigated in future.

ACKNOWLEDGEMENTS
This work was supported by the National Basic Research Program of China (973 Program) (2013CB934001), National Natural Science Foundation of China (51074011 and 51274017) and National 863 Program (2007AA03Z231 and 2011AA11A257).

References

1. U. Kasavajjula, C. Wang, and A. J. Appleby, J. Power Sources., 163 (2006) 1003.
2. M. Holzapfel, H. Buqa, L. J. Hardwick, M. Hahn, A. Würsig, W. Scheifele, P. Novák, R. Kötz, C. Veit, and F-M. Petrat, Electrochim. Acta., 52 (2006) 973.
3. R. Teki, M. K. Datta, R. Krishnan, T. C. Parker, T.-M. Lu, P. N. Kumta, and N. Koratkar, Small., 5 (2009) 2236.

4. Z. S. Wen, J. Yang, B. F. Wang, K. Wang, Y. Liu, Electrochem. Commun. 5 (2003) 165.
5. J. P. Maranchi, A. F. Hepp, A. G. Evans, N. T. Nuhfer, and P. N. Kumta, J. Electrochemical Soc., 153 (2006) A1246.
6. X. L. Yang, Z. Y. Wen, X. X. Xu, B. Lin, and Z. X. Lin, J. Electrochemical Soc., 153 (2006) A1341.
7. J. C. Guo, and C. S. Wang, Chemical Commun., 46 (2010) 1428.
8. Z. B. Zhou, Y. H. Xu, W. G. Liu, and L. B. Niu, J. Alloys and Compounds., 493 (2010) 636.
9. J. Y. Xiang, X. L. Wang, X. H. Xia, L. Zhang, Y. Zhou, S. J. Shi, and J. P. Tu, Electrochim. Acta., 55 (2010) 4921.
10. I. Prakash, P. Muralidharan, N. Nallamuthu, M. Venkateswarlu, and N. Satyanarayana, Mater. Res. Bulletin., 42 (2007) 1619.
11. J. Lia, J. R. Dahn, J. Electrochem. Soc., 154 (2007) 156.
12. B. Key, R. Bhattacharyya, M. Morcrette, V. Seznec, J. M. Tarascon, C. P. Grey, J. AM. CHEM. SOC, 131 (2009) 9239.
13. J. Y. Xiang, J. P. Tu, Y. F. Yuan, X. L. Wang, X. H. Huang, Z.Y. Zeng, Electrochim. Acta., 54 (2009) 1160.
14. Y. M. Lee, J. Y. Lee, H.T. Shim, J. K. Lee, J. K. Park, J. Electrochem. Soc.., 154 (2007) 515.
15. Y. C. Yen, S. C. Chao, H. C. Wu, N. L. Wu, J. Electrochem. Soc., 156 (2009) 95.
16. C. Q. Zhang, J. P. Tu, X. H. Huang, Y. F. Yuan, X. T. Chen, F. Mao, J. Alloys and Compounds., 441 (2007) 52.
17. L. B. Chen, J. Y. Xie, H. C. Yu, T. H. Wang, J. Appl. Electrochem., 39 (2009) 1157.
18. V. A.Sethuraman, K. Kowolik, V. Srinivasan, J. Power Sources., 196 (2011) 393.
19. J.Y. Song, H.H. Lee, Y.Y. Wang, C.C. Wan, J. Power Sources., 111 (2002) 255.
20. R. Ruffo, S. S. Hong, C. K. Chan, R. A. Huggins, Y. Cui, J. Phys. Chem. C., 113 (2009) 11390.
21. J. Guo, A. Sun, X. Chen, C. Wang, A. Manivannan, Electrochimica Acta., 56 (2011) 3981.
22. H. Wu, G. Zheng, N. Liu, T. J. Carney, Y. Yang, Y. Cui, Nano Letters., 12 (2012) 904.
23. S. Hwang, C. Cho, H. Kim, Electrochimica Acta., 55 (2010) 3236.
24. V. G. Khomenko, V. Z. Barsukov, J. E. Doninger, I. V. Barsukov, J. Power Sources., 165 (2007) 598.